Long-term Temozolomide Treatment Induces Marked Amino Metabolism Modifications and an Increase in TMZ Sensitivity in Hs683 Oligodendroglioma Cells[1]

Delphine Lamoral-Theys[*,2], Marie Le Mercier[†,2,3], Benjamin Le Calvé[†,3], Michal A. Rynkowski[‡], Céline Bruyère[†], Christine Decaestecker[†,3], Benjamin Haibe-Kains[§,¶], Gianluca Bontempi[¶], Jacques Dubois[*], Florence Lefranc[†,‡,3] and Robert Kiss[†,3]

*Laboratoire de Chimie Bioanalytique, Toxicologie et Chimie Physique Appliquée, Brussels, Belgium; †Laboratoire de Toxicologie, Département de Bioanalyse et Toxicologie Pharmaceutique, Institut de Pharmacie, Brussels, Belgium; ‡Service de Neurochirurgie, Hôpital Erasme, Brussels, Belgium; §Functional Genomics Unit, Institut Jules Bordet, Brussels, Belgium; ¶Machine Learning Group, Department of Computer Science, Université Libre de Bruxelles, Brussels, Belgium

Abstract

Gliomas account for more than 50% of all primary brain tumors. The worst prognosis is associated with gliomas of astrocytic origin, whereas gliomas with an oligodendroglial origin offer higher sensitivity to chemotherapy, especially when oligodendroglioma cells display 1p19q deletions. Temozolomide (TMZ) provides therapeutic benefits and is commonly used with radiotherapy in highly malignant astrocytic tumors, including glioblastomas. The actual benefits of TMZ during long-term treatment in oligodendroglioma patients have not yet been clearly defined. In this study, we have investigated the effects of such a long-term TMZ treatment in the unique Hs683 oligodendroglioma model. We have observed increased TMZ sensitivity of Hs683 orthotopic tumors that were previously treated in vitro with months of progressive exposure to increasing TMZ concentrations before being xenografted into the brains of immunocompromised mice. Whole-genome and proteomic analyses have revealed that this increased TMZ sensitivity of Hs683 oligodendroglioma cells previously treated for long periods with TMZ can be explained, at least partly, by a TMZ-induced p38-dependant dormancy state, which in turn resulted in changes in amino acid metabolism balance, in growth delay, and in a decrease in Hs683 oligodendroglioma cell-invasive properties. Thus, long-term TMZ treatment seems beneficial in this Hs683 oligodendroglioma model, which revealed itself unable to develop resistance against TMZ.

Neoplasia (2010) 12, 69–79

Introduction

Gliomas are the most common primary brain malignancy found in adults and include astrocytomas, oligodendrogliomas, and ependymomas [1,2]. Current recommendations are that patients with high-grade astrocytomas should undergo maximum surgical resection, followed by concurrent radiation and chemotherapy with the alkylating drug temozolomide (TMZ). Indeed, since the clinical trial published in 2005 by Stupp et al., concomitant and adjuvant chemoradiotherapy with TMZ has become the standard treatment of high-grade gliomas from astroglial origin [3,4]. This treatment is now also widely used to treat oligodendrogliomas [5]. Moreover, patients whose oligodendroglioma displays 1p/19q chromosome deletions can be safely treated with single-agent TMZ [6,7].

TMZ belongs to the triazene family of compounds, which are a group of alkylating agents whose mechanism of antitumor effects is mediated in part through DNA methylation of O(6)-guanine [8]. The biologic end point of TMZ-induced antitumor effects in glioma cells relates to apoptosis-related cell death [9,10]. TMZ also exerts marked antiangiogenic effects in experimental gliomas [11,12].

Gliomas, including oligodendroglioma, can develop TMZ resistance, which can be partly mediated by O(6)-methylguanine-DNA methyltransferase (MGMT), which demethylates TMZ-methylated guanosine [13,14]. When treated with TMZ, glioma cells also defend themselves through proautophagic mechanisms [15,16], which, if remain sustained, lead to apoptosis [9,10]. Glioma cells become sensitized to TMZ treatment, resulting in increased apoptosis, when Na^+/H^+ exchanger regulating factor 1 expression is reduced [17].

However, the cellular effects induced by long-term treatment (LTT) of oligodendroglioma cells with TMZ remain unknown. The present study aimed to characterize such long-term TMZ treatment under *in vitro* and *in vivo* experimental conditions in the human Hs683 oligodendroglioma model. The validation of the oligodendroglial origin of the Hs683 model has been performed in several steps: Hs683 tumor cells are 1p19q codeleted [18] and are sensitive to proapoptotic chemotherapy [18] and to TMZ [11,19,20] under *in vivo* orthotopic brain xenograft conditions. Moreover, Hs683 cells display high levels of expression of integrin β_4 [21] as human biopsy oligodendrogliomas do [21,22]. Hs683 cells do not express the human 1p-distal ATAD 3B gene, which is highly expressed in astroglioma cells [23]. Finally, they contain only one Notch2 gene copy per diploid genome as seen in oligodendrogliomas [24], in which loss of the 1p centromeric marker within intron 12 of the Notch2 gene is associated with a favorable prognosis in oligodendroglioma patients [25]. Lastly, we have shown that BEX2 (the brain-expressed X-linked gene) interferes with Hs683 oligodendroglioma cell biology in a manner that markedly differs from what is observed in astrocytic tumors [26]. As illustrated in the Results section (Figure 1), Hs683 orthotopic xenografts developing in the brains of immunocompromised mice display highly invasive properties. Thus, the Hs683 oligodendroglioma model might correspond to the few glioblastomas displaying an oligodendroglial origin [27] and/or component [28].

In the present study, Hs683 oligodendroglioma cells have been cultured for months in incremental concentrations of TMZ until Hs683 cells were able to grow in culture medium containing 1 mM TMZ. Before long-term adaptation, the native (preadaptation) TMZ-related *in vitro* IC_{50} value (i.e., the concentration that decreases by 50% the growth of glioma cells after 3 days of culture in presence of TMZ) ranges between 100 and 300 μM [11,15,29]. Whole-genome analyses have been performed in Hs683 cells left untreated (and thereafter named TMZ-sensitive, i.e., TMZ-S Hs683 cells) and in long-term TMZ-treated (TMZ-LTT) Hs683 cells. TMZ-S and TMZ-LTT Hs683 cells have also been orthotopically grafted into the brain of immunocompromised mice, and the effects of chronic TMZ treatments have been analyzed.

Materials and Methods

Cell Cultures and Compounds

The human Hs683 oligodendroglioma (ATCC code HTB-138), U373 (ATCC code HTB-17) and T98G (ATCC code CRL-1690) astroglioma, and HT-29 colon cancer (ATCC code HTB-38) cell lines were obtained from the American Type Culture Collection (ATCC, Manassas, VA) and maintained in our laboratory as detailed previously [11,18–21].

In Vitro Long-term Treatment of Hs683 Oligodendroglioma Cells with TMZ

Hs683 cells either have been left untreated (TMZ-S Hs683 cells) or were cultured for months in incremental concentrations of TMZ (TMZ-LTT Hs683 cells). Firstly, they were cultured with 100 nM TMZ for 4 weeks, then with 1 μM TMZ for 5 weeks, then with 10 μM TMZ for 12 weeks, then with 100 μM TMZ for 12 weeks, and finally with 1 mM TMZ for 4 weeks. TMZ-LTT Hs683 cells were then cultivated for 8 weeks without TMZ treatment (washout) before *in vivo* orthotopic grafting and genomic analyses. We choose this 8-week period of washout to investigate as whether TMZ-LTT Hs683 cells retained differences in terms of biologic characteristics compared with Hs683 cells left untreated with TMZ. This means that the selection pressure exerted by TMZ was partially undone.

In Vivo Orthotopic Grafting of Hs683 Oligodendroglioma Cells into the Brains of immunocompromised Mice

TMZ-S and TMZ-LTT Hs683 tumor cells were grafted orthotopically into the brains of nude mice as described previously [18–21]. In each experiment, all mice (8-week-old female *nu/nu* mice; 21-23 g; Iffa Credo, Charles Rivers, Arbresle, France) had 100,000 Hs683 cells implanted on the same day into the left temporal lobe. Mice were then treated or not with TMZ (80 mg/kg per os) three times per week for 3 weeks starting at day 5 after graft. Each experimental group contained 11 mice. All the *in vivo* experiments described in the present study were performed on the basis of Authorization No. LA1230509 of the Animal Ethics Committee of the Federal Department of Health, Nutritional Safety and the Environment (Belgium).

In Vitro *Determination of Mitotic Rates*

The number of mitotic cells in TMZ-S *versus* TMZ-LTT Hs683 cells was characterized *in vitro*. Cells were followed for 72 hours, and mitotic cells were detected manually on pictures on the basis of their characteristic roundness and brightness. The data were expressed as a total number of mitotic cells counted at the 24th, 48th, and 72nd hours after plating on a 1-mm² area. For each condition, 12 microscopic fields of 1 mm² each on three replicates have been analyzed.

In Vitro *Determination of Apoptotic Rates*

Apoptotic rates in TMZ-S *versus* TMZ-LTT Hs683 cells were determined using flow cytometry after annexin V staining. Hs683 cells were harvested by trypsinization, resuspended in serum-containing medium to neutralize the trypsin, and washed twice with PBS. Cells were then

resuspended in ice-cold 1× binding buffer (Sigma-Aldrich, Bornem, Belgium) at a density of 10^6 cells/ml and stained with 5 µl of annexin V–fluorescein isothiocyanate and 10 µl of propidium iodide (PI; Sigma-Aldrich) as described previously [30]. The fluorescence was analyzed immediately on a Cell Lab Quanta flow cytometer (Beckman Coulter Analis, Suarlee, Belgium) equipped with a 488-nm argon laser.

In Vitro *Determination of Hs683 Cell Invasive Features*

Invasive features of Hs683 cells *in vitro* were assessed by means of the Boyden transwell invasion system (BD BioCoat Matrigel invasion

chambers; BD Biosciences Discovery Labware, Bedford, MA) as detailed elsewhere [31].

Genomic and Proteomic Analyses

Genomic analyses.   Total RNA was extracted from TMZ-S Hs683-S or TMZ-LTT Hs683-LTT (after 8 weeks of washout), and the quality and integrity of the extracted RNA were assessed as detailed previously [31,32]. Full-genome analyses were performed at the VIB Microarray Facility (UZ Gasthuisberg, Catholic University of Leuven, Leuven, Belgium) using the Affymetrix Human Genome U133 set Plus 2.0 (High Wycombe, UK). Microarray data analyses were undertaken as detailed previously [19,20].

Protein expression measurements.   Western blot analyses were performed as detailed previously [21,31,33]. Equal loading was verified by the bright Ponceau red coloration of the membranes, and the integrity and quantity of the extracts were assessed by means of tubulin immunoblot analysis. The following primary antibodies were used for Western blot analysis: anti-Grp78 (dilution 1:1000; Sigma-Aldrich), anti-GADD34 (dilution 1:500; Santa Cruz Biotechnology, Tebu-bio, Boechout, Belgium), anti-ATF4 (dilution 1:100; Santa Cruz Biotechnology), anti–branched chain amino acid 1 (BCAT1, dilution 1:100; BD Biosciences, Erembodegem, Belgium), anti-phosphoserine aminotransferase 1 (PSAT1, dilution 1:1000: Sigma-Aldrich), anti–phospho-p38 mitogen-activated protein kinase (MAPK, dilution 1:250; Cell Signaling Technology, Bioké, Leiden, The Netherlands). Secondary antibodies were purchased from Pierce (PerbioScience, Erembodegem, Belgium). Western blots were developed using the Pierce Supersignal Chemiluminescence system.

Reverse Transcription–Polymerase Chain Reaction

The procedure used for the standard reverse transcription–polymerase chain reaction (RT-PCR) was identical to that described previously [31,32]. The following primers were used: vimentin forward 5′-gattcag-gaacagcatgtc-3′ and reverse 5′-tctctagtttcaaccgtctta-3′, CK20 forward 5′-gaacctaaatgaccgtctagc-3′ and reverse 5′-ccaaatctgttttatgtaagggttag-3′, CD44 forward 5′-ggcttagacagagttgatct-3′ and reverse 5′-ggctatgagacttg-tatcactac-3′, CD133 forward 5′-gagagtaactaggattctagctt-3′ and reverse
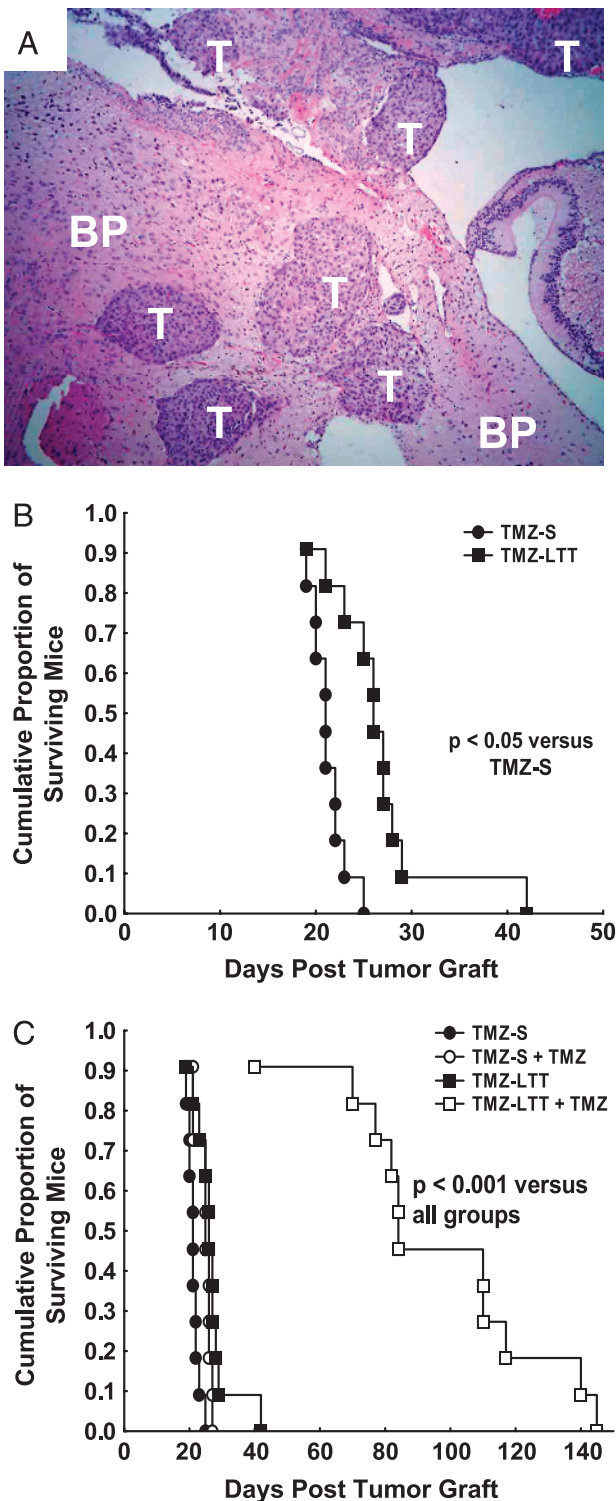
Figure 1. (A) Morphologic illustration (hematoxylin-eosin staining, ×40) of a TMZ-S Hs683 oligodendroglioma xenograft in the brain of an immunocompromised mouse after having orthotopically injected 10^5 TMZ-S Hs683 tumor cells 17 days earlier. *T* indicates tumor; BP, brain parenchyma. (B) Survival of immunocompromised mice with brain xenografts of TMZ-S (black circles) *versus* TMZ-LTT (black squares) Hs683 oligodendroglioma cells. Mice have been orthotopically grafted into their brains with 10^5 Hs683 tumor cells on day 0 (D0). Hs683 oligodendroglioma cell populations that have been left untreated with TMZ are labeled as TMZ-S Hs683 cells, whereas Hs683 oligodendroglioma cells that have been able to grow *in vitro* over months in the presence of 1 mM TMZ have been labeled TMZ-LTT Hs683 cells (see Materials and Methods). (C) Survival of immunocompromised mice with brain xenografts of TMZ-S Hs683 cells treated (open circles) or not (black circles) with TMZ compared to TMZ-LTT Hs683 cells treated (open squares) or not (black squares) with TMZ. The TMZ treatment (80 mg/kg per os) was given three times a week (Monday, Wednesday, Friday) during three consecutive weeks, with treatment starting at D5.
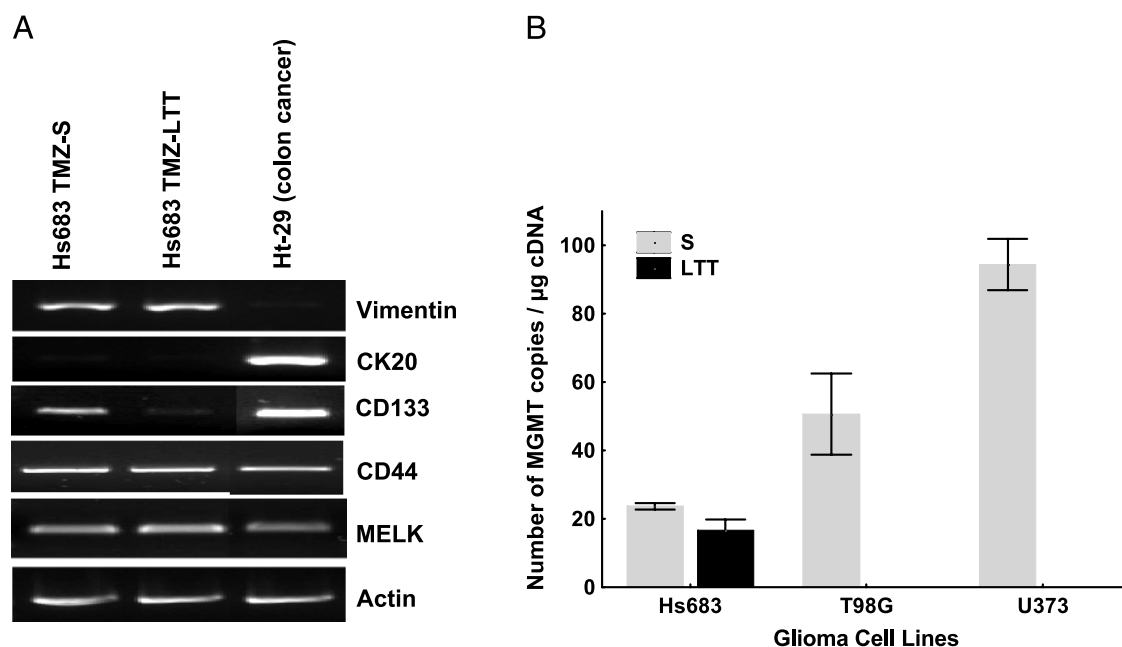
Figure 2. (A) mRNA expression (RT-PCR analyses) of vimentin, cytokeratin 20 (CK20), CD133, MELK, and CD44 in Hs683 oligodendroglioma cell populations that have been left untreated (TMZ-S Hs683 cells) or that have been able to grow *in vitro* over months in the presence of 1 mM TMZ (TMZ-LTT Hs683 cells; see Materials and Methods). HT-29 colon cancer cells have been used as an internal control. Actin RT-PCR was used as a quality control for the reverse transcription and the PCR. (B) Quantitative determination of MGMT mRNA expression (quantitative RT-PCR) in TMZ-S *versus* TMZ-LTT Hs683 oligodendroglioma cells. Wild-type U373 and T98G astroglioma cells [11,18,21] have been chosen as internal references.

5′-ccattcgacgatagtacttagc-3′, MELK forward 5′-gtgaatccagatcaactgttg-3′ and reverse 5′-gctagataggatgtcttccacta-3′, and actin forward 5′-ctaagtca-tagtccgcctag-3′ and reverse 5′-aaatcgtgcgtgacattaagg-3′. The PCR conditions for all primer pairs, except actin, were predenaturation (4 minutes at 94°C), PCR amplification (35 cycles at 94°C for 30 seconds [denaturation], 59°C for 30 seconds [annealing], 72°C for 1 minute [extension]), and final extension (1 cycle at 72°C for 10 minutes). For actin, the PCR conditions were predenaturation (4 minutes at 94°C), PCR amplification (25 cycles at 94°C for 30 seconds [denaturation], 62°C for 30 seconds [annealing], 72°C for 1 minute [extension]), and final extension (1 cycle at 72°C for 10 minutes).

Quantitative RT-PCR has been performed in TMZ-S and TMZ-LTT Hs683 oligodendroglioma cells to determine the levels of MGMT expression. The following primers were used: forward GCGCACCG-TTTGCGACTTGG and reverse GCACTGCATCAGGGGCTCCG (35 cycles at 60°C).

Statistical Analyses

Survival analyses were carried out by means of Kaplan-Meier curves that were compared with the log-rank test. Statistical comparisons between TMZ-S and TMZ-LTT groups were established by carrying out the nonparametric Mann-Whitney test. All the statistical analyses were realized using Statistica (Statsoft, Tulsa, OK).

Results

Chronic *In Vivo* Treatment of TMZ-S and TMZ-LTT Hs683 Orthotopic Oligodendroglioma Xenografts with TMZ

The Hs683 oligodendroglioma model is biologically aggressive as illustrated in Figure 1A. Indeed, the orthotopic injection of 10^5 Hs683

cells only into the brains of immunocompromised mice leads to the development of highly invasive tumors (T; Figure 1A) everywhere in the brain parenchyma (BP; Figure 1A).

Hs683 cells that have never been cultured in the presence of TMZ (TMZ-S Hs683 cells) and Hs683 cells that have been rendered capable of growth *in vitro* in the presence of 1 mM TMZ (TMZ-LTT Hs683 cells) were orthotopically grafted (10^5 cells per graft) into the brains of immunocompromised mice. The data in Figure 1B show that TMZ-LTT Hs683 oligodendroglioma-bearing mice survived significantly ($P < .05$) longer than TMZ-S Hs683 oligodendroglioma-bearing ones. Moreover, whereas TMZ treatment only slightly, nevertheless, significantly ($P < .05$), increased the survival of TMZ-S Hs683 oligodendroglioma-bearing mice, it markedly ($P < .001$) increased the survival of TMZ-LTT Hs683 oligodendroglioma-bearing ones (Figure 1C). We observed no morphologic differences between histologically analyzed TMZ-LTT *versus* TMZ-S Hs683 tumors (data not shown).

Characterization of Cancer Stem Cell Profiles in TMZ-LTT versus TMZ-S Hs683 Oligodendroglioma Cells

Beier et al. [34] have recently demonstrated that TMZ induces a dose- and time-dependent decline of the stem cell subpopulation (i.e., CD133+ cells) in various experimental glioma models. We have thus analyzed the expression of CD133 as well as other stem cells markers such as CD44, nestin, and the maternal embryonic leucine zipper kinase (MELK) [35,36] in TMZ-LTT Hs683 cells compared with TMZ-S cells. The RT-PCR analyses (Figure 2A) revealed that CD44, nestin, and MELK patterns of expression are similar in Hs683 TMZ-S *versus* TMZ-LTT cells. In contrast, long-term TMZ treatment eliminated CD133+ Hs683 cells (Figure 2A). These data thus perfectly fit in with those reported by Beier et al. [34]. The human HT-29 colon cancer

cells were used as a reference cell population illustrating the absence of vimentin and the presence of cytokeratin CK20 expression in these cells (Figure 2).

Characterization of MGMT Expression in TMZ-S versus TMZ-LTT Hs683 Oligodendroglioma Cells

As indicated in the Introduction, it is well known that glioma cells acquire resistance to TMZ for a longitudinal treatment by overexpressing MGMT. The data in Figure 2*B* show that TMZ-LTT Hs683 cells do not overexpress MGMT, at least at the mRNA levels, when compared with TMZ-S Hs683 cells.

Genomic and Proteomic Analyses of TMZ-LTT versus TMZ-S Hs683 Oligodendroglioma Cells

To partly decipher how long-term TMZ *in vitro* treatment of Hs683 oligodendroglioma cells confers this model with marked increased TMZ sensitivity *in vivo* (Figure 1), we made use of a whole human genome analysis. The expression levels of 1447 genes were found to be increased or decreased at least two-fold in TMZ-LTT compared with TMZ-S Hs683 cells. We then subjected this list of 1447 genes to a functional analysis using the Expression Analysis Systematic Explorer software package (Ease, version 2.0) [37]. This software gathers biologic information on the genes and identifies statistically overrepresented functional categories within a given list of genes. The significantly overrepresented functional categories extracted from this series of 1447 genes were all related to amino acid metabolism (Table 1). Indeed, there were 36 genes (of 1447) involved in amino acid metabolism whose expression was impaired in TMZ-LTT Hs683 cells compared to TMZ-S Hs683 cells (Table 2).

Figure 3 illustrates the data obtained at the protein level with respect to 2 of the 36 genes listed in Table 2, that is, *BCAT1* (cytosolic) and *PSAT1*. These two genes are involved in amino acid metabolism and have been shown to play a role in tumor cell growth [38,39], apoptosis [40], and chemoresistance [41]. Western blot analyses show that TMZ-LTT Hs683 cells overexpressed BCAT1 and PSAT1 proteins compared with TMZ-S Hs683 cells (Figure 3). This increased expression of BCAT1 and PSAT1 proteins was not observed when TMZ-S Hs683 cells were challenged *in vitro* with a single 100-μM TMZ treatment for 72 hours (Figure 3), a feature that suggests the necessity for prolonged TMZ challenges of Hs683 cells to observe *BCAT1* and *PSAT1* expression increases.

Table 2 reveals that long-term TMZ treatment decreases *BCAT1* and *PSAT1* expression at the mRNA levels in Hs683 oligodendroglioma cells, whereas Figure 3 illustrates an increase of BCAT1 and PSAT1 expression at the protein levels during long-term TMZ treatment. These apparent contradictory data therefore suggest that, whereas long-term TMZ treatment decreases the transcriptional activity of various genes implicated in amino acid metabolism (including *BCAT1* and *PSAT1*), such a decrease in transcriptional activity—that could be translated as an "alarm signal" by Hs683 cells—activates the translation of preexisting mRNA into proteins.

The endoplasmic reticulum stress response (ERSR) actively contributes in defending cells in general and cancer cells in particular when these cells face adverse effects. Further analysis of the list of the 1447 genes whose expressions were modified in TMZ-LTT Hs683 cells compared with TMZ-S Hs683 cells revealed that many genes in this list are indeed involved in the ERSR process, including several genes coding for chaperones proteins and for components of the PKR-like endoplasmic reticulum kinase (PERK) signaling pathway (Table 3). ERSR activation and especially the PERK signaling pathway (Figure 4*A*) has been demonstrated to modulate the expression of genes involved in amino acid metabolism, including *PSAT1* and *BCAT1* [41,42]. Moreover, the activation of the PERK signaling pathway by the MAPK p38 kinase was also shown to modulate tumor cell dormancy (Figure 4*A*) [43], a feature that could explain the increase of survival of TMZ-LTT Hs683 oligodendroglioma-bearing mice compared with the TMZ-S Hs683 oligodendroglioma-bearing ones (Figure 1*C*). We have thus analyzed the expression levels of several components and targets of the PERK signaling pathway, as well as the activation level of p38 MAPK. As illustrated in Figure 4*B*, the protein expression levels of Grp78, ATF4, and GADD34 were not modified in TMZ-LTT Hs683 cells compared to TMZ-S Hs683 cells. In contrast, the phosphorylation level of the MAPK p38 kinase was increased in TMZ-LTT compared with TMZ-S Hs683 cells, suggesting a constitutive activation of p38 MAPK in TMZ-LTT compared with TMZ-S Hs683 cells (Figure 4*B*). A single TMZ *in vitro* treatment of 100 μM for 72 hours did not activate p38 MAPK (Figure 4*B*), a feature that is identical to what we observed for BCAT1 and PSAT1 protein expression (Figure 3).

Altogether these data thus suggest that long-term TMZ *in vitro* treatment of Hs683 cells could push them in a tumor cell dormancy state through constitutive p38 MAPK activation, without activation of the PERK signaling pathway. We further investigated this hypothesis as detailed below.

Table 1. Gene Categories Overrepresented in the Set of Genes Detected as Differentially Expressed in TMZ-LTT Compared with TMZ-S Hs683 Cells.

System	Gene Category	List		Population		Ease Score	Bootstrap Score
		Hits	Total	Hits	Total		
Biologic process	Amine metabolism	36	588	328	10,937	0.00008	0.006
Biologic process	Amino acid and derivative metabolism	32	588	290	10,937	0.0002	0.01
Biologic process	Amine biosynthesis	14	588	80	10,937	0.0003	0.02
Biologic process	Amino acid metabolism	27	588	252	10,937	0.001	0.07

System refers to the system of categorizing genes (e.g., "Biologic process") in the databases provided by the Ease software package.
Gene Category refers to the specific category of genes within the System (e.g., "Amine metabolism").
List Hits refers to the number of genes in the list of differentially expressed genes (list_diff resulting from the microarray data analysis) that belong to the Gene Category.
List Total refers to the number of genes in list_diff that belong to any Gene Category within the System.
Population Hits is the number of genes in the total group of genes assayed (list_tot) that belong to the specific Gene Category.
Population Total refers to the number of genes in list_tot that belong to any Gene Category within the System.
The *EASE* score is the probability value characterizing the change of proportion between the two ratios: population hits/population total and list hits/list total. It constitutes the upper band of the distribution of leave-one-out Fisher exact probabilities computed on these two ratios.
The *Bootstrap* method is an iteratively running overrepresentation analysis on random gene lists to determine true probability more accurately.

Table 2. Amino Acid Metabolism–Related Gene Whose Expression Is Modified in TMZ LTT Hs683 Cells.

Gene Symbol	Gene Name	Hs683 TMZ-S	Hs683 TMZ-LTT	Ratio TMZ-S/TMZ-LTT
Genes downregulated in TMZ-LTT Hs683 cells				
HPD	4-Hydroxyphenylpyruvate dioxygenase	258	15	12.9
BCAT1	Branched chain aminotransferase 1, cytosolic	345	25	12.8
CPS1	Carbamoyl-phosphate synthetase 1, mitochondrial	1849	277	5.2
CBS	Cystathionine-β-synthase	263	56	4.3
PSAT1	Phosphoserine aminotransferase 1	3735	996	3.7
WARS	Tryptophanyl-tRNA synthetase	1074	286	3.5
GFPT1	Glutamine-fructose-6-phosphate transaminase 1	1822	495	3.4
SLC3A1	Solute carrier family 3, member 1	28	8	3.3
PSPH	Phosphoserine phosphatase	564	174	3.2
ASNS	Asparagine synthetase	4167	1214	3.2
IDS	Iduronate 2-sulfatase (Hunter syndrome)	215	65	3.1
CTPS	CTP synthase	878	295	3.0
WWOX	WW domain containing oxidoreductase	190	66	2.9
GSTZ1	Glutathione transferase zeta 1 (maleylacetoacetate isomerase)	253	92	2.6
MARS	Methionine-tRNA synthetase	1988	768	2.6
AARS	Alanyl-tRNA synthetase	2875	1014	2.5
HYOU1	Hypoxia-upregulated 1	1624	535	2.5
GAMT	Guanidinoacetate N-methyltransferase	111	43	2.5
ARSJ	Arylsulfatase family, member J	74	18	2.5
ARG2	Arginase, type II	77	26	2.4
CARS	Cysteinyl-tRNA synthetase	537	203	2.3
DIO1	Deiodinase, iodothyronine, type I	22	9	2.2
AGMAT	Agmatine ureohydrolase (agmatinase)	258	96	2.1
HSD17B6	Hydroxysteroid (17-β) dehydrogenase 6	32	14	2.1
ABAT	4-Aminobutyrate aminotransferase	48	20	2.1
PHGDH	Phosphoglycerate dehydrogenase	785	348	2.1
GARS	Glycyl-tRNA synthetase	4951	2247	2.0
DDC	Dopa decarboxylase (aromatic L-amino acid decarboxylase)	277	131	2.0
Genes upregulated in TMZ-LTT Hs683 cells				
GLCE	Glucuronic acid epimerase	247	885	0.30
SULT1C1	Sulfotransferase family, cytosolic, 1C, member 1	10	33	0.30
ARHGAP24	Rho GTPase activating protein 24	76	201	0.4
ASS1	Argininosuccinate synthetase	1642	4745	0.4
HAL	Histidine ammonia-lyase	13	70	0.4
KDELC1	KDEL (Lys-Asp-Glu-Leu) containing 1	130	314	0.4
MAOA	Monoamine oxidase A	11	33	0.5
SULT1A1	Sulfotransferase family, cytosolic, 1A, member 1	634	1452	0.5

In Vitro *Characterization of Growth Kinetics (Proliferation versus Apoptosis) and Invasion Properties of TMZ-LTT versus TMZ-S Hs683 Oligodendroglioma Cells*

Tumor cell dormancy is a phenomenon often related to sustain ERSR process that arise due to either cell cycle arrest or a dynamic equilibrium state in which cell proliferation is in balance with cells un-dergoing death (usually apoptosis). We have thus analyzed the mitotic and apoptotic rates in TMZ-S and TMZ-LTT Hs683 cells. The data illustrated in Figure 5 show that TMZ-LTT Hs683 cells display weaker proliferative activity (Figure 5A) and higher apoptosis (and also necrosis) levels (Figure 5B) than TMZ-S Hs683 cells. In addition, Boyden chamber assay revealed that TMZ-LTT Hs683 cells display
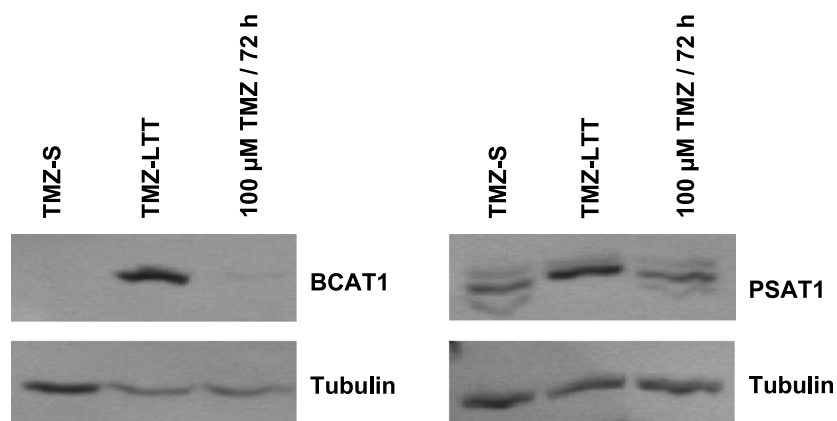

Figure 3. Western blot analysis of BCAT1 and PSAT1 expression in Hs683 oligodendroglioma cell populations that have been left untreated (TMZ-S Hs683 cells) or that have been able to grow *in vitro* over months in the presence of 1 mM TMZ(TMZ-LTT Hs683 cells; see Materials and Methods), and in TMZ-S Hs683 cells treated with 100 μM TMZ for 72 hours. Tubulin was used as quality and loading control.

Table 3. ER Stress–Related Gene Whose Expression Is Modified in TMZ LTT Hs683 Cells.

Gene Symbol	Gene Name	Hs683 TMZ-S	Hs683 TMZ-LTT	Ratio TMZ-S/TMZ-LTT
PERK signaling pathway				
HSP5A (Grp78)	Heat shock 70 kDa protein 5 (glucose-regulated protein, 78 kDa)	14,912	6873	0.46
EIF2AK3 (PERK)	Eukaryotic translation initiation factor 2-α kinase 3	937	440	0.47
DDIT3 (CHOP)	DNA damage–inducible transcript 3	1613	239	0.15
PPP1R15A (GADD34)	Protein phosphatase 1, regulatory (inhibitor) subunit 15A	370	165	0.44
EIF5	Eukaryotic translation initiation factor 5	3332	819	0.24
EIF4BP1	Eukaryotic translation initiation factor 4E binding protein 1	1630	676	0.41
EIF4BP2	Eukaryotic translation initiation factor 4E binding protein 2	72	190	2.58
Chaperones				
HYOU1 (ORP150)	Hypoxia-upregulated 1	1624	534	0.32
DNAJBA1	DnaJ (Hsp40) homolog, subfamily A, member 1	564	1492	2.64
DNAJB9 (MDG1)	DnaJ (Hsp40) homolog, subfamily B, member 9	2019	404	0.20
DNAJB11	DnaJ (Hsp40) homolog, subfamily B, member 11	2690	1224	0.41
DNAJB13	DnaJ (Hsp40) related, subfamily B, member 13	97	38	0.39
DNAJC6	DnaJ (Hsp40) homolog, subfamily C, member 6	257	84	0.32
DNAJC12	DnaJ (Hsp40) homolog, subfamily C, member 12	178	861	4.83
DNAJC15	DnaJ (Hsp40) homolog, subfamily C, member 15	24	81	3.37
HSPA8	Heat shock 70 kDa protein 8	2146	5006	2.33
HSPA1A	Heat shock 70 kDa protein 1A	835	3390	4.06
HSPA1B	Heat shock 70 kDa protein 1B	208	1070	5.14

weaker ($P < .01$) invasive properties than TMZ-S Hs683 tumor cells (Figure 5*C*).

Discussion

TMZ is an alkylating agent that is part of most current therapeutic regimens for highly malignant gliomas, including not only glioblastomas [3,4,44] but also highly malignant oligodendrogliomas [5–7]. This is the first report on TMZ LTT of human oligodendroglioma cells with the use of the Hs683 experimental oligodendroglioma as a model. However, the current study relies on *in vitro* experiments: *in vitro* long-term exposure of glioma cells to TMZ is not an identical condition to *in vivo* longitudinal treatment. We thus envisage in future experiments to analyze gene expression profiles in astroglioma and oligodendroglioma xenografts as well as in biopsies from glioma patients who benefited from long-term TMZ treatment.

We observed in the current study that Hs683 oligodendroglioma cells that have been treated over months *in vitro* with TMZ (the Hs683 cell line that we labeled TMZ-LTT Hs683 cells in the present study) are slightly, nevertheless, significantly less aggressive biologically than Hs683 cells that have been left untreated (the Hs683 cell line that we labeled TMZ-S Hs683 cells in the present study), a feature that we observed both *in vitro* (Figure 5) and *in vivo* (Figure 1). We found that treating immunocompromised mice bearing orthotopic xenografts of TMZ-LTT *versus* TMZ-S Hs683 cells with the same TMZ regimen showed markedly higher therapeutic benefits of TMZ in TMZ-LTT Hs683-bearing mice than in TMZ-S ones (Figure 1).

Gliomas contain both progenitor (stem) cells (cancer stem cells, CSCs) and differentiated malignant cells [35,36]. Beier et al. [34] have recently demonstrated that TMZ induces a dose- and time-dependent decline of the stem cell subpopulation (i.e., CD133+ cells) in various experimental glioma models. The data illustrated in Figure 2 perfectly fit in with those reported by Beier et al. [34]. Indeed, we also observed an almost complete disappearance of CD133+ CSCs in TMZ-LTT Hs683 tumor populations compared with TMZ-S ones. Beier et al. [34] also claimed that their data strongly suggest that optimized TMZ-based chemotherapeutic protocols might substantially improve the elimination of GBM stem cells and, consequently, prolong the survival of patients, knowing that CSCs may be uniquely responsible for GBM re-

currence [34]. Our data illustrated in Figure 1 fully support conclusions drawn by Beier et al. [34] about optimized TMZ-based chemotherapy prolonging the survival of glioma patients. The fact that CD133 expression disappeared with long-term TMZ treatment, whereas CD44 expression did not (Figure 2), could appear surprising at first glance because both markers are usually considered as stem cell markers. In fact, CD44 is a glial progenitor marker [45], whereas CD133 is a marker for a subset of leukemia and GBM CSCs [46]. CD133 GBM-positive cells are resistant to chemotherapeutic agents, including TMZ [46]. The current data thus indicate that long-term TMZ treatment eliminated CD133-positive stem cells in Hs683 oligodendroglioma cell populations (increasing, therefore, their sensitivity to TMZ), whereas not modifying the glial nature of these cell populations (the maintenance of CD44 positivity).

Apart from diminishing the proportion of CSC *versus* more differentiated cell subpopulations in gliomas [34] (and our current data), TMZ could also provide therapeutic benefits during LTT of gliomas by modifying the levels of expression of various gene products displaying proangiogenic and promigratory influences in glioma cell populations. For example, we have demonstrated that chronic *in vitro* exposure to increasing concentrations of TMZ decreases the expression levels of hypoxia-inducible factor-1α, inhibitor of DNA binding/differentiation proteins 1 and 2, and cMyc in various experimental gliomas [11]. All these factors have been shown to play major roles in angiogenesis and adaptation to hypoxic metabolism [11]. We have performed in the current study a whole-genome expression analysis comparing TMZ-S *versus* TMZ-LTT Hs683 cell populations and discovered that the long-term TMZ treatment of Hs683 oligodendroglioma cells markedly modified gene patterns of expression of a large set of genes involved in amino acid metabolism. There is growing evidence that metabolic enzymes can in fact directly contribute to carcinogenesis [47]. Moreover, it has been shown that amino acid imbalance inhibits the growth of gastric carcinoma cells *in vitro* [48]. Our results show that LTT of Hs683 oligodendroglioma cells with TMZ increases the protein expression of BCAT1 and PSAT1. PSAT1 is implicated in catabolism: it catalyzes the second reaction step in the biosynthesis of the amino acid serine [38]. The overexpression of PSAT1 was shown to stimulate cell growth and increases chemoresistance of colon cancer cells [38]. BCAT1 is one of the enzymes that regulate the first step in the degradation

of branched chain amino acids. The overexpression of BCAT1 has been shown to lead to a decrease in cell viability [40] and the depletion of BCAT1 was shown to block cell proliferation [48]. We showed that whereas long-term TMZ treatment decreased BCAT1 and PSAT1 expression at the mRNA levels in Hs683 oligodendroglioma cells (Table 2), it increased BCAT1 and PSAT1 expression at the protein levels in these tumor cells (Figure 3). We suggest that it is the TMZ-induced decrease in BCAT1 and PSAT1 transcriptional activity that induces an increase in BCAT1 and PSAT1 translational activity by TMZ-attacked Hs683 tumor cells as a mechanism of defense of Hs683 tumor cells against TMZ if one refers to the procarcinogenic effects already described for PSAT1 [39] as well as for its protective effects in cancer cells facing chemotherapy-related adverse effects [38]. It has also been demonstrated that, at the mRNA level, PSAT1 is a pre-dictor of tamoxifen therapy response in steroid hormone receptor–positive patients with recurrent breast cancer [49].

The molecular circuit that activates BCAT1 and PSAT1 translational activity by TMZ while their transcriptional activity is partially impaired by TMZ remains to be identified, but we suspect the ERSR and the unfolded protein response (UPR) to be both involved in this process. Indeed, we previously observed that glioma cells are able to defend themselves against TMZ by overexpressing, for example, galectin-1, which displays marked proangiogenic [20,26] and promigratory [50,51] effects in glioma cells. We showed that reducing galectin-1 expression in TMZ-treated glioma cells significantly increases the therapeutic benefits contributed by TMZ in the Hs683 oligodendroglioma model [19]. We observed that these events were related to modifications occurring at the molecular level of both the ERSR and the UPR
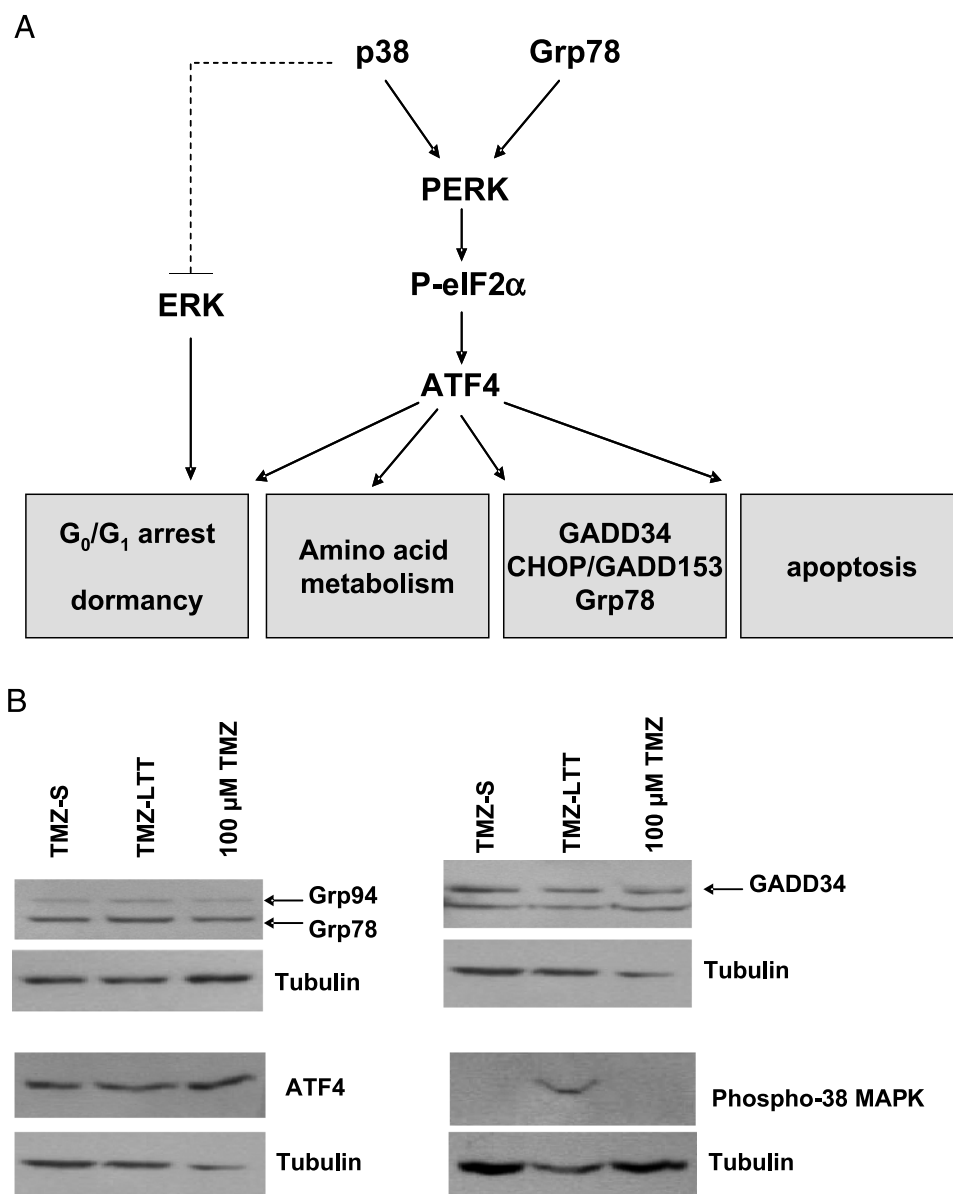

Figure 4. (A) PERK activation by Grp78 under stress condition lead to the phosphorylation of eIF2α, which activates the translation of the transcription factor ATF4, which in turn regulates gene expression in response to environmental stresses; p38 MAPK activation induces growth arrest and tumor cell dormancy through the activation of PERK and also through the suppression of ERK signaling. (B) Western blot analyses of Grp78, Grp94, GADD34, ATF4, and phospho-p38 MAPK expression in TMZ-S *versus* TMZ-LTT Hs683 cells and in TMZ-S Hs683 cells treated with 100 μM TMZ for 72 hours (see the legend to Figure 3). Tubulin was used as a quality and loading control.
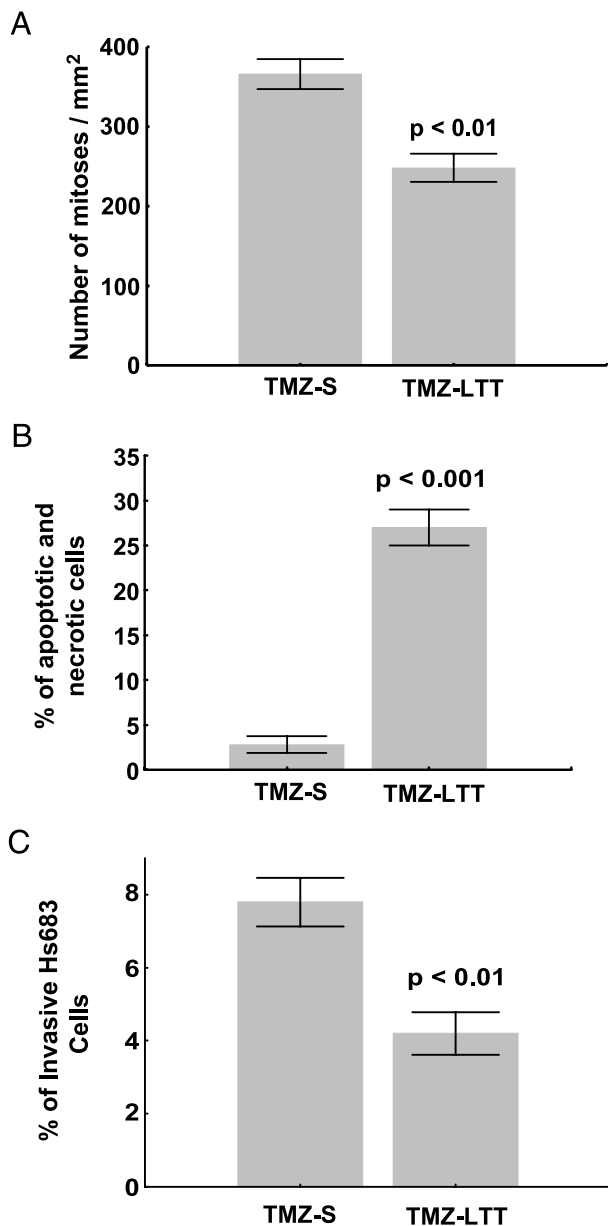
Figure 5. (A) Quantitative determination of the percentage of mitotic cells during 72 hours in Hs683 oligodendroglioma cell populations that have been left untreated (TMZ-S Hs683 cells) or that have been able to grow *in vitro* over months in the presence of 1 mM TMZ (TMZ-LTT Hs683 cells; see Materials and Methods). (B) Flow cytometry analysis of double-stained (Annexin V and PI) TMZ-S and TMZ-LTT Hs683 cells. Apoptotic cells include annexin V$^+$/PI$^-$ (early apoptosis) and annexin V$^+$/PI$^+$ (late apoptosis), whereas necrotic cells are annexin V$^-$/PI$^+$ and normal cells annexin V$^-$/PI$^-$. (C) Characterization of the invasiveness of TMZ-S and TMZ-LTT Hs683 cells cultured for 24 hours in Matrigel-coated Boyden chambers. Data are illustrated in A to C as mean ± SEM values, and all experiments have been carried out in triplicate.

processes [19,20]. Harding et al. [42] have shown that the integrated stress response pathway initiated by the activation of PERK (Figure 4A) regulates amino acid metabolism and resistance to oxidative stress. These authors have compared the profile of genes expressed in unstressed and in ER-stressed wild type, ATF4–/–, and PERK–/– mouse embryonic fibroblast. They observed that the ATF4–/– and PERK–/–

cells were severely impaired in activating genes involved in amino acid import and metabolism [42]. Moreover, Lecca et al. [41] have shown that UPR induces the coordinated transcriptional activation of genes encoding proteins involved in the synthesis and the transport of amino acid. These authors have thus suggested that the amino acid response might be a component of the UPR [41].

We further demonstrate in the current study that LTT of Hs683 oligodendroglioma cells with TMZ induces constitutive activation of the stress activated MAP kinase p38 (Figure 4B). The p38 MAPK activates the PERK signaling pathway, which in turn induces growth arrest and tumor cell dormancy [43]. The fact that we did not observe TMZ-induced activation of the PERK signaling pathway at the protein levels (Figure 4B), whereas we observed TMZ-induced constitutive activation of p38 MAPK (Figure 4B), suggests that the long-term TMZ treatment could induce a dormancy state in Hs683 oligodendroglioma cells through signaling pathways that would involve ERK and/or NF-κB [52]. It is postulated that the stress-dependent activation of p38 may eliminate cells through apoptosis but that the cells that are able to cope with stress may resume growth or enter a p38-dependent state of dormancy [43,53,54]. Results in the current study seem to fit with this hypothesis. Indeed, the LTT of Hs683 cells with TMZ induced a reduction in the percentage of mitotic cells and an increase in the percentage of apoptotic cells (Figure 5). Moreover, we have also observed that the TMZ-LTT Hs683 cells were significantly less aggressive biologically *in vivo* than the TMZ-S Hs683 cells (Figure 1), a feature that could also relate to TMZ-induced dormancy state.

The dormancy state is usually associated with drug resistance [43,54]; however, in our model, the LTT of Hs683 cells with TMZ before their grafting in the brain of immunocompromised mice seems to render them more sensitive to TMZ treatment (Figure 1D). Thus, if TMZ actually induces a dormancy state in Hs683 cells, this dormancy state seems only partial.

To conclude, we hypothesize that LTT of Hs683 oligodendroglioma cells with TMZ induces a moderate p38-dependant dormancy state, resulting in a metabolic change, a growth delay, and a decrease in invasive properties in these long-term TMZ-treated Hs683 tumor cells with, as a general consequence, a marked increased sensitivity to further TMZ treatment in these cells when transplanted *in vivo*.

Acknowledgments

References

[1] Louis DN (2006). Molecular pathology of malignant gliomas. *Annu Rev Pathol* **1**, 97–117.

[2] Louis DN, Ohgaki H, Wiestler OD, and Cavenee WK (2007). *WHO Classification of Tumours of the Central Nervous System.* Lyon, France: International Agency for Research on Cancer (IARC).

[3] Stupp R, Mason WP, van den Bent MJ, Weller M, Fisher B, Taphoorn MJ, Belanger K, Brandes AA, Marosi C, Bogdahn U, et al. (2005). Radiotherapy plus concomitant and adjuvant temozolomide for glioblastoma. *N Engl J Med* **352**, 987–996.

[4] Stupp R, Hegi ME, Gilbert MR, and Chakravarti A (2007). Chemoradiotherapy in malignant glioma: standard of care and future directions. *J Clin Oncol* **25**, 4127–4136.

[5] Abrey LE, Louis DN, Paleologos N, Lassman AB, Raizer JJ, Mason W, Finlay J, MacDonald DR, DeAngelis LM, and Cairncross JG (2007). Survey of treatment recommendations for anaplastic oligodendroglioma. *Neuro Oncol* **9**, 314–318.

[6] Mikkelsen T, Doyle T, Anderson J, Margolis J, Paleologos N, Gutierrez J, Croteau D, Hasselbach L, Avedissian R, and Schultz L (2009). Temozolomide single-agent chemotherapy for newly diagnosed anaplastic oligodendroglioma. *J Neurooncol* **92**, 57–63.

[7] Bromberg JE and van den Bent MJ (2009). Oligodendrogliomas: molecular biology and treatment. *Oncologist* **14**, 155–163.

[8] Marchesi F, Turriziani M, Tortorelli G, Avvisati G, Torino F, and De Vecchis L (2007). Triazene compounds: mechanism of action and related DNA repair systems. *Pharmacol Res* **56**, 275–287.

[9] Roos WP, Batista LF, Naumann SC, Wick W, Weller M, Menck CF, and Kaina B (2007). Apoptosis in malignant glioma cells triggered by the temozolomide-induced DNA lesion O_6-methylguanine. *Oncogene* **26**, 186–197.

[10] Takagi Y, Hidaka M, Sanada M, Yoshida H, and Sekiguchi M (2008). Different initial steps of apoptosis induced by two types of antineoplastic drugs. *Biochem Pharmacol* **76**, 303–311.

[11] Mathieu V, De Neve N, Le Mercier M, Dewelle J, Gaussin JF, Dehoux M, Kiss R, and Lefranc F (2008). Combining bevacizumab with temozolomide increases the antitumor efficacy of temozolomide in a human glioblastoma orthotopic xenograft model. *Neoplasia* **10**, 1383–1392.

[12] Kim JT, Kim JS, Ko KW, Kong DS, Kang CM, Kim MH, Son MJ, Song HS, Shin HJ, Lee DS, et al. (2006). Metronomic treatment of temozolomide inhibits tumor cell growth through reduction of angiogenesis and augmentation of apoptosis in orthotopic models of gliomas. *Oncol Rep* **16**, 33–39.

[13] Hegi ME, Diserens AC, Godard S, Dietrich PY, Regli L, Ostermann S, Otten P, Van Melle G, de Tribolet N, and Stupp R (2004). Clinical trial substantiates the predictive value of *O-6*-methylguanine-DNA methyltransferase promoter methylation in glioblastoma patients treated with temozolomide. *Clin Cancer Res* **10**, 1871–1874.

[14] Wick W, Platten M, and Weller M (2009). New (alternative) temozolomide regimens for the treatment of glioma. *Neuro Oncol* **11**, 69–79.

[15] Kanzawa T, Germano IM, Komata T, Ito H, Kondo Y, and Kondo S (2004). Role of autophagy in temozolomide-induced cytotoxicity for malignant glioma cells. *Cell Death Differ* **11**, 448–457.

[16] Katayama M, Kawaguchi T, Berger MS, and Pieper RO (2007). DNA damaging agent–induced autophagy produces a cytoprotective adenosine triphosphate surge in malignant glioma cells. *Cell Death Differ* **14**, 548–558.

[17] Kislin KL, McDonough WS, Eschbacher JM, Armstrong BA, and Berens ME (2009). NHERF-1: modulator of glioblastoma cell migration and invasion. *Neoplasia* **11**, 377–387.

[18] Branle F, Lefranc F, Camby I, Jeuken J, Geurts-Moespot A, Sprenger S, Sweep F, Kiss R, and Salmon I (2002). Evaluation of the efficiency of chemotherapy in *in vivo* orthotopic models of human glioma cells with and without 1p19q deletions and in C6 rat orthotopic allografts serving for the evaluation of surgery combined with chemotherapy. *Cancer* **95**, 641–655.

[19] Le Mercier M, Lefranc F, Mijatovic T, Debeir O, Haibe-Kains B, Bontempi G, Decaestecker C, Kiss R, and Mathieu V (2008). Evidence of galectin-1 involvement in glioma chemoresistance. *Toxicol Appl Pharmacol* **229**, 172–183.

[20] Le Mercier M, Mathieu V, Haibe-Kains B, Bontempi G, Mijatovic T, Decaestecker C, Kiss R, and Lefranc F (2008). Knocking down galectin 1 in human hs683 glioblastoma cells impairs both angiogenesis and endoplasmic reticulum stress responses. *J Neuropathol Exp Neurol* **67**, 456–469.

[21] Belot N, Rorive S, Doyen I, Lefranc F, Bruyneel E, Dedecker R, Micik S, Brotchi J, Decaestecker C, Salmon I, et al. (2001). Molecular characterization of cell substratum attachments in human glial tumors relates to prognostic features. *Glia* **36**, 375–390.

[22] Ikota H, Kinjo S, Yokoo H, and Nakazato Y (2006). Systematic immunohistochemical profiling of 378 brain tumors with 37 antibodies using tissue microarray technology. *Acta Neuropathol* **111**, 475–482.

[23] Hubstenberger A, Labourdette G, Baudier J, and Rousseau D (2008). ATAD 3A and ATAD 3B are distal 1p-located genes differentially expressed in human glioma cell lines and present *in vitro* anti-oncogenic and chemoresistant properties. *Exp Cell Res* **314**, 2870–2883.

[24] Sivasankaran B, Degen M, Ghaffari A, Hegi ME, Hamou MF, Ionescu MC, Zweifel C, Tolnay M, Wasner M, Mergenthaler S, et al. (2009). Tenascin-C is a novel RBPJκ-induced target gene for Notch signaling in gliomas. *Cancer Res* **69**, 458–465.

[25] Boulay JL, Miserez AR, Zweifel C, Sivasankaran B, Kana V, Ghaffari A, Luyken C, Sabel M, Zerrouqi A, Wasner M, et al. (2007). Loss of NOTCH2 positively predicts survival in subgroups of human glial brain tumors. *PLoS ONE* **2**, e576.

[26] Le Mercier M, Fortin S, Mathieu V, Roland I, Spiegl-Kreinecker S, Haibe-Kains B, Bontempi G, Decaestecker C, Berger W, Lefranc F, et al. (2009). Galectin-1 pro-

[27] Decaestecker C, Camby I, Gordower L, De Witte O, Cras P, Martin JJ, Pasteels JL, Van Ham P, Brotchi J, Kiss R, et al. (1998). Characterization of astroglial *versus* oligodendroglial phenotypes in glioblastomas by means of quantitative morphonuclear variables generated by computer-assisted microscopy. *J Neuropathol Exp Neurol* **57**, 791–802.

[28] He J, Mokhtari K, Sanson M, Marie Y, Kujas M, Huguet S, Leuraud P, Capelle L, Delattre JY, Poirier J, et al. (2001). Glioblastomas with an oligodendroglial component: a pathological and molecular study. *J Neuropathol Exp Neurol* **60**, 863–871.

[29] Fisher T, Galanti G, Lavie G, Jacob-Hirsch J, Kventsel I, Zeligson S, Winkler R, Simon AJ, Amariglio N, Rechavi G, et al. (2007). Mechanisms operative in the antitumor activity of temozolomide in glioblastoma multiforme. *Cancer J* **13**, 335–344.

[30] Dumont P, Ingrassia L, Rouzeau S, Ribaucour F, Thomas S, Roland I, Darro F, Lefranc F, and Kiss R (2007). The Amaryllidaceae isocarbostyril narciclasine induces apoptosis by activation of the death receptor and/or mitochondrial pathways in cancer cells but not in normal fibroblasts. *Neoplasia* **9**, 766–776.

[31] Mathieu V, Mijatovic T, van Damme M, and Kiss R (2005). Gastrin exerts pleiotropic effects on human melanoma cell biology. *Neoplasia* **7**, 930–943.

[32] Megalizzi V, Mathieu V, Mijatovic T, Gailly P, Debeir O, De Neve N, Van Damme M, Bontempi G, Haibe-Kains B, Decaestecker C, et al. (2007). 4-IBP, a sigma1 receptor agonist, decreases the migration of human cancer cells, including glioblastoma cells, *in vitro* and sensitizes them *in vitro* and *in vivo* to cytotoxic insults of proapoptotic and proautophagic drugs. *Neoplasia* **9**, 358–369.

[33] Mijatovic T, Mathieu V, Gaussin JF, De Neve N, Ribaucour F, Van Quaquebeke E, Dumont P, Darro F, and Kiss R (2006). Cardenolide-induced lysosomal membrane permeabilization demonstrates therapeutic benefits in experimental human non–small cell lung cancers. *Neoplasia* **8**, 402–412.

[34] Beier D, Rohrl S, Pillai DR, Schwarz S, Kunz-Schughart LA, Leukel P, Proescholdt M, Brawanski A, Bogdahn U, Trampe-Kieslich A, et al. (2008). Temozolomide preferentially depletes cancer stem cells in glioblastoma. *Cancer Res* **68**, 5706–5715.

[35] Lee da Y and Gutmann DH (2007). Cancer stem cells and brain tumors: uprooting the bad seeds. *Expert Rev Anticancer Ther* **7**, 1581–1590.

[36] Sanai N, Alvarez-Buylla A, and Berger MS (2005). Neural stem cells and the origin of gliomas. *N Engl J Med* **353**, 811–822.

[37] Hosack DA, Dennis G Jr, Sherman BT, Lane HC, and Lempicki RA (2003). Identifying biological themes within lists of genes with EASE. *Genome Biol* **4**, R70.

[38] Vie N, Copois V, Bascoul-Mollevi C, Denis V, Bec N, Robert B, Fraslon C, Conseiller E, Molina F, Larroque C, et al. (2008). Overexpression of phosphoserine aminotransferase PSAT1 stimulates cell growth and increases chemoresistance of colon cancer cells. *Mol Cancer* **7**, 14.

[39] Zhou W, Feng X, Li H, Wang L, Zhu B, Zhang H, Yao K, and Ren C (2007). Functional evidence for a nasopharyngeal carcinoma-related gene *BCAT1* located at 12p12. *Oncol Res* **16**, 405–413.

[40] Eden A and Benvenisty N (1999). Involvement of branched-chain amino acid aminotransferase (Bcat1/Eca39) in apoptosis. *FEBS Lett* **457**, 255–261.

[41] Lecca MR, Wagner U, Patrignani A, Berger EG, and Hennet T (2005). Genome-wide analysis of the unfolded protein response in fibroblasts from congenital disorders of glycosylation type-I patients. *FASEB J* **19**, 240–242.

[42] Harding HP, Zhang Y, Zeng H, Novoa I, Lu PD, Calfon M, Sadri N, Yun C, Popko B, Paules R, et al. (2003). An integrated stress response regulates amino acid metabolism and resistance to oxidative stress. *Mol Cell* **11**, 619–633.

[43] Ranganathan AC, Adam AP, Zhang L, and Aguirre-Ghiso JA (2006). Tumor cell dormancy induced by p38^{SAPK} and ER-stress signaling: an adaptive advantage for metastatic cells? *Cancer Biol Ther* **5**, 729–735.

[44] Stupp R, Hegi ME, Mason WP, van den Bent MJ, Taphoorn MJ, Janzer RC, Ludwin SK, Allgeier A, Fisher B, Belanger K, et al. (2009). Effects of radiotherapy with concomitant and adjuvant temozolomide *versus* radiotherapy alone on survival in glioblastoma in a randomized phase III: 5-year analysis of the EORTC-NCIC trial. *Lancet Oncol* **10**, 459–466.

[45] Rebetz J, Tian D, Persson A, Widegren B, Salford LG, Englund E, Gisselsson D, and Fan X (2008). Glial progenitor-like phenotype in low-grade glioma and enhanced CD133-expression and neuronal lineage differentiation potential in high-grade glioma. *PLoS ONE* **3**, e1936.

[46] Liu G, Yuan X, Zeng Z, Tunici P, Ng H, Abdulkadir IR, Lu L, Irvin D, Black KL, and You JS (2006). Analysis of gene expression and chemoresistance of CD133$^+$ cancer stem cells in glioblastoma. *Mol Cancer* **5**, 67.

angiogenic and promigratory effects in the Hs683 oligodendroglioma model are partly mediated through the control of BEX2 expression. *Neoplasia* **11**, 485–496.

[47] Vander Heiden MG, Cantley LC, and Thompson CB (2009). Understanding the Warburg effect: the metabolic requirements of cell proliferation. *Science* **324**, 1029–1033.

[48] Sun X, Zhang N, Li K, Liu M, Zhi X, Jiang X, and Shou N (2003). Branched chain amino acid imbalance selectively inhibits the growth of gastric carcinoma cells *in vitro*. *Nutr Res* **23**, 1279–1290.

[49] Martens JW, Nimmrich I, Koenig T, Loop MP, Harbeck N, Model F, Kluth A, Bolt-de Vries J, Sieuwerts AM, Portengen H, et al. (2005). Association of DNA methylation of phosphoserine aminotransferase with response to endocrine therapy in patients with recurrent breast cancer. *Cancer Res* **65**, 4101–4417.

[50] Camby I, Belot N, Lefranc F, Sadeghi N, de Launoit Y, Kaltner H, Musette S, Darro F, Danguy A, Salmon I, et al. (2002). Galectin-1 modulates human glioblastoma cell migration into the brain through modifications to the actin cytoskeleton and levels of expression of small GTPases. *J Neuropathol Exp Neurol* **61**, 585–596.

[51] Fortin S, Le Mercier M, Camby I, Spiegl-Kreinecker S, Berger W, Lefranc F, and Kiss R (in press). Galectin-1 is implicated in the protein kinase C epsilon/vimentin–controlled trafficking of integrin-β_1 in glioblastoma cells. *Brain Pathol*.

[52] Bulavin DV and Fornace AJ Jr (2004). p38 MAP kinase's emerging role as a tumor suppressor. *Adv Cancer Res* **92**, 95–118.

[53] Aguirre-Ghiso JA, Estrada Y, Liu D, and Ossowski L (2003). ERK(MAPK) activity as a determinant of tumor growth and dormancy; regulation by p38(SAPK). *Cancer Res* **63**, 1684–1695.

[54] Udagawa T (2008). Tumor dormancy of primary and secondary cancers. *APMIS* **116**, 615–628.